ISME

Nonlinear Vibration of Functionally Graded Cylindrical Shells under Radial Harmonic Load

M. Tavakolian*
PhD Student

A.A. Jafari†
Ph.D

S.M.R. Khalili‡
Ph.D

In this paper, the nonlinear vibration of functionally graded (FGM) cylindrical shells subjected to radial harmonic excitation is investigated. The nonlinear formulation is based on a Donnell's nonlinear shallow-shell theory, in which the geometric nonlinearity takes the form of von Karman strains. The Lagrange equations of motion were obtained by an energy approach. In order to reduce the system to finite dimensions, the middle surface displacements were expanded by using trial functions. These functions were expressed in terms of Fourier series containing linear mode shapes, which were obtained from free vibration analysis. The large-amplitude response and amplitude frequency curves of shell were computed by using numerical method for both linear and nonlinear analysis.

Keyword: nonlinear vibration, functionally graded, harmonic load

1 Introduction

FGMs are microscopically inhomogeneous materials, in which the mechanical properties vary smoothly and continuously from one surface to the other. This is achieved by continuous change in composition of the FGMs. Composition is varied with continuous change in the volume fraction of constituent materials. Material properties of the FGMs are tailored with the variation of the volume fraction of the constituent materials. These materials are considered as potential structural materials for the space crafts [1–4]. These graded materials are introduced by Shiota [5] and Koizumi [6]. Usually these materials are made from a mixture of ceramic and metal(s) with a continuously varying volume fraction [2, 6–9]. The advantages of using these materials are that they can withstand thermal shocks while maintaining structural integrity. Ceramic constituent of the material provides the high temperature resistance while the metal part prevents the fracture caused by high stresses. Studies on FGMs have been extensive but are largely confined to analysis of thermal stress, deformation and fracture [10–15].
In addition to the linear analyses (small strains), the nonlinear response of FGMs has also attracted research interest. Praveen and Reddy [16] conducted a geometrically nonlinear

* Corresponding Author, Ph.D Student, Centre of Excellence for Research in Advanced Materials and Structures, Faculty of Mechanical Engineering, K.N. Toosi University of Technology, Tehran, matavakolian@gmail.com

† Ph.D, Centre of Excellence for Research in Advanced Materials and Structures, Faculty of Mechanical Engineering, K.N. Toosi University of Technology, Tehran, jafari@uast.ac.ir

‡ Ph.D, Centre of Excellence for Research in Advanced Materials and Structures, Faculty of Mechanical Engineering, K.N. Toosi University of Technology, Tehran, smrkhalili2005@gmail.com

transient analysis of FGM plates under thermal and mechanical loading, and Park and Kim [17] carried out a thermal post buckling and vibration analysis of FGM plates based on the first-order shear deformation plate theory. Reddy [18] proposed a theoretical formulation for FGM plates using the third-order shear deformation plate theory, and developed a corresponding finite element model that accounts for thermomechanical coupling, time dependency, and von Ka´rma´n type geometric nonlinearity. Yang et al. [19] presented a formulation for the thermomechanical post buckling analysis of FGM shell panels based on the classical shell theory with von Ka´rma´ n–Donnell type nonlinearity, and Hosseini Kordkheili and Naghdabadi [20] derived a finite element formulation for the geometrically non- linear thermoelastic analysis of FGM plates and shells using the updated Lagrangian approach. Arciniega and Reddy [21] presented a tensor-based finite element formulation for the large deformation analysis of FGM shells, and Woo and Merguid [22] reported an analytical solution for the coupled large deflection of FGM plates and shallow shells under a mechanical load and in a temperature field. The nonlinear post buckling behaviors of functionally graded cylindrical shells (FGCSs) under uniform radial pressure and torsion load are investigated by using the nonlinear large deflection theory of cylindrical shells [23, 24].
In the present work, analytical studies on the non-linear dynamic of simply supported, circular cylindrical shells composed of functionally graded material under periodic radial loading is presented. The properties were graded in the thickness direction according to a volume fraction power law distribution. The linear mode shapes and natural frequencies were obtained by using linear analysis. In this study, the middle surface displacements were expanded by using trial functions. These functions were expressed in terms of Fourier series containing linear mode shapes, which were obtained from free vibration analysis. The Lagrange equations were used to reduce nonlinear partial differential equations to a set of ordinary differential equations, from the potential and kinetic energies, and the virtual work of the external forces, and then these equations were solved by using numerical method. Numerical results of the amplitude-frequency for both linear and nonlinear analysis were obtained. The effects of external load on the nonlinear frequency response were investigated. The influence of material composition (power law exponent) and load value on the dynamic response was investigated. Other studies and FEM analysis were used for verification of the result.

2 Fundamental equations

As shown in figure (1), consider a functionally graded cylindrical shell, with length L and radius R and simply supported boundary conditions. The shell of the FGM considered is assumed to be of uniform thickness h.

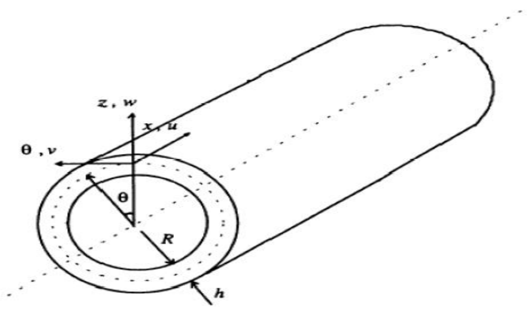

Figure 1 The geometry of a FG cylindrical shell

In order to accurately model the material properties of FGMs, the properties must be both temperature and position dependent. This is achieved by using a simple rule of mixtures for the stiffness parameters coupled with the temperature dependent properties of the constituents. The volume fraction is spatial function and the properties of the constituents are functions of the temperature. The combination of these functions gives rise to the effective material properties of FGMs and can be expressed as [25]:

$$F_{eff}(T,z) = F_c(T)V(z) + F_m(T)\big(1 - V(z)\big) \tag{1}$$

In which F_{eff} is the effective material property of FGMs, F_c and F_m are the temperature dependent properties of the ceramic and metal respectively, and V is the volume fraction of FGMs. In addition, a simple power law exponent of the volume fraction distribution is used to provide a measure of the amount of ceramic and metal in FGMs. In the present case, the volume fraction is defined as [25]:

$$V(z)=\left(\frac{z+h/2}{h}\right)^{\beta} \tag{2}$$

Where β is the power law exponent $(0 \le \beta \le \infty)$. The equation of motion according to Donnell's theory can be written as:

$$N_{x,x}+\frac{1}{R}N_{x\theta,\theta}+F_x=\rho_t u_{,tt} \tag{3}$$

$$N_{\theta x,x}+\frac{1}{R}N_{\theta,\theta}+F_\theta=\rho_t v_{,tt} \tag{4}$$

$$M_{x,xx}+\frac{2}{R}M_{x\theta,x\theta}+\frac{1}{R^2}M_{\theta,\theta\theta}-\frac{1}{R}N_\theta+F_z=\rho_t w_{,tt} \tag{5}$$

Where:

$$\rho_t=\int_{-h/2}^{h/2}\rho dz \tag{6}$$

The stress and moment resultant is defined as:

$$\begin{Bmatrix} N_x \\ N_\theta \\ N_{x\theta} \\ M_x \\ M_\theta \\ M_{x\theta} \end{Bmatrix}=\begin{bmatrix} A_{11} & A_{12} & A_{16} & B_{11} & B_{12} & B_{16} \\ A_{12} & A_{22} & A_{26} & B_{12} & B_{22} & B_{26} \\ A_{16} & A_{26} & A_{66} & B_{16} & B_{26} & B_{66} \\ B_{11} & B_{12} & B_{16} & D_{11} & D_{12} & D_{16} \\ B_{12} & B_{22} & B_{26} & D_{12} & D_{22} & D_{26} \\ B_{16} & B_{26} & B_{66} & D_{16} & D_{26} & D_{66} \end{bmatrix}\begin{Bmatrix} e_1 \\ e_2 \\ \gamma \\ k_1 \\ k_2 \\ \tau \end{Bmatrix} \tag{7}$$

Where:

$$\left(A_{ij},B_{ij},D_{ij}\right)=\int_{-h/2}^{h/2}Q_{ij}\left(1,z,z^2\right)dz \quad (i,j=1,2,6) \tag{8}$$

and

$$Q_{11}=Q_{22}=\frac{E_{eff}}{1-\nu_{eff}^2} \tag{9}$$

$$Q_{12}=\nu_{eff}\frac{E_{eff}}{1-\nu_{eff}^2} \tag{10}$$

$$Q_{66}=\frac{E_{eff}}{2(1+\nu_{eff})} \tag{11}$$

$$Q_{16}=Q_{26}=0 \tag{12}$$

Where E_{eff} and ν_{eff} are the effective elastic modulus and effective Poisson's ratio of the functionally graded shell, respectively, and are accounted according to Eq. (1)-(2). The strain components e_x, e_θ and $e_{x\theta}$ which are the strains in the x-direction, the circumferential direction and the shear strain in the xθ-plane of the middle surface, respectively, can be expressed as:

$$\begin{Bmatrix} e_x \\ e_\theta \\ e_{x\theta} \end{Bmatrix}=\begin{Bmatrix} e_1 \\ e_2 \\ \gamma \end{Bmatrix}+z\begin{Bmatrix} k_1 \\ k_2 \\ \tau \end{Bmatrix} \tag{13}$$

The linear deflection and curvatures are defined by Donnell's theory as:

$$e_1=\frac{\partial u}{\partial x} \tag{14}$$

$$e_2=\frac{1}{R}\left(\frac{\partial v}{\partial \theta}+w\right) \tag{15}$$

$$\gamma=\frac{1}{R}\frac{\partial u}{\partial \theta}+\frac{\partial v}{\partial x} \tag{16}$$

$$k_1=-\frac{\partial^2 w}{\partial x^2} \tag{17}$$

$$k_2=-\frac{1}{R^2}\frac{\partial^2 w}{\partial \theta^2} \tag{18}$$

$$\tau=-\frac{2}{R}\frac{\partial^2 w}{\partial x\partial \theta} \tag{19}$$

The nonlinear strain-displacement relations for the large deflection by Donnell's theory are:

$$e_1=\frac{\partial u}{\partial x}+\frac{1}{2}\left(\frac{\partial w}{\partial x}\right)^2 \tag{20}$$

$$e_2=\frac{1}{R}\left(\frac{\partial v}{\partial \theta}+w\right)+\frac{1}{2R^2}\left(\frac{\partial w}{\partial \theta}\right)^2 \tag{21}$$

$$\gamma=\frac{1}{R}\frac{\partial u}{\partial \theta}+\frac{\partial v}{\partial x}+\frac{1}{R}\frac{\partial w}{\partial x}\frac{\partial w}{\partial \theta} \tag{22}$$

3 Linear vibration

The boundary conditions for the cylindrical shell, which is simply supported along its curve edges at x = 0 and x = L, are considered as:

$$w = v = M_x = N_x = 0 \quad \text{at } x = 0, \tag{23}$$

In order to satisfy the boundary conditions, u, v and w are defined by the following double Fourier series [26]:

$$u = \sum_m \sum_n \bar{A}_{mn} T_{mn}(t) = \sum_m \sum_n A_{mn} \frac{d\eta_u(x)}{dx} \cos(n\theta) T_{mn}(t) \tag{24}$$

$$v = \sum_m \sum_n \bar{B}_{mn} T_{mn}(t) = \sum_m \sum_n B_{mn} \eta_v(x) \sin(n\theta) T_{mn}(t) \tag{25}$$

$$w = \sum_m \sum_n \bar{C}_{mn} T_{mn}(t) = \sum_m \sum_n C_{mn} \eta_w(x) \cos(n\theta) T_{mn}(t) \tag{26}$$

$$\eta_i(x) = \alpha_1 \cosh\left(\frac{\lambda_m x}{L}\right) + \alpha_2 \cos\left(\frac{\lambda_m x}{L}\right) - \sigma_m \left(\alpha_3 \sinh\left(\frac{\lambda_m x}{L}\right) - \alpha_4 \sin\left(\frac{\lambda_m x}{L}\right)\right) \quad (i = u, v, w) \tag{27}$$

In Eq. (24)-(26), $T_{mn}(t)$ is function of time. Also A_{mn}, B_{mn} and C_{mn} are the constant coefficients of the natural mode shapes associated with the free vibration problems, m is the axial half wave number and n is the circumferential wave number. Values of α_i, σ_m and λ_m in Eq. (27) could be obtained from corresponding boundary conditions

$$\alpha_1 = \alpha_2 = \alpha_3 = 0, \quad \alpha_4 = 1, \ \sigma_m = 1, \quad \lambda_m = m\pi \tag{28}$$

To solve the free vibration analysis the function of time is treated as$T_{mn}(t) = e^{i\omega_{mn}(t)}$, Where ω_{mn} is the natural frequency. By considering external loads (F_x, F_θ, F_z) equal to zero in Eq. (3)-(5), natural frequencies and mode shapes are obtained. By applying a Galerkin method, the following set of equations is derived as follows:

$$\left[[K_{ij}] - \omega_{mn}^2 [M_{ij}]\right] \{A_{mn}\ B_{mn}\ C_{mn}\}^T = 0 \qquad (i, j = 1, .., 3) \tag{29}$$

Where K_{ij}, M_{ij} are stiffness and mass matrices. By setting determinant of coefficients equal to zero, the characteristic frequency equation is derived as:

$$\delta_1 \omega^6 + \delta_2 \omega^4 + \delta_3 \omega^2 + \delta_4 = 0 \tag{30}$$

Where δ_i are constant coefficients. By solving Eq. (30), natural frequencies are calculated, and by substituting these frequencies in Eq. (29), the constant coefficients of mode shapes are obtained.

For linear dynamic response analysis the applied loads are defined as:

$$F_z(x, \theta, t) = P(x, \theta) f(t) = \sum_m \sum_n P_{mn} \sin\left(\frac{m\pi x}{L}\right) \cos(n\theta) f(t) \tag{31}$$

In the above equations, $f(t)$ is function of time P_{mn} is the constant coefficient that can be calculated from applied loads. Substituting the displacements and assumed exciting forces and moments in the equilibrium equations, and using the results of free vibration we have:

$$-\rho_t\overline{A}_{mn}\omega_{mn}^2 T_{mn}(t) = \rho_t\overline{A}_{mn}\ddot{T}_{mn}(t) \tag{32}$$

$$-\rho_t\overline{B}_{mn}\omega_{mn}^2 T_{mn}(t) = \rho_t\overline{B}_{mn}\ddot{T}_{mn}(t) \tag{33}$$

$$-\rho_t\overline{C}_{mn}\omega_{mn}^2 T_{mn}(t) = \rho_t\overline{C}_{mn}\ddot{T}_{mn}(t) - F_z(x,\theta,t) \tag{34}$$

After summation of two sides of the above equation and simplifying, we find a second order ordinary differential equation as follows:

$$\ddot{T}_{mn}(t) + \omega^2{}_{mn}(t)T_{mn}(t) = G_{mn}(t) \tag{35}$$

$$G_{mn}(t) = \frac{C_{mn}(t)P_{mn}f(t)}{(A^2{}_{mn}+B^2{}_{mn}+C^2{}_{mn})\rho_t} \tag{36}$$

For zero initial conditions, the solution of Eq. (35) will be obtained by using Laplace transformation.

4 Nonlinear vibration

Most of studies on large-amplitude (geometrically nonlinear) vibrations of circular cylindrical shells used Donnell’s nonlinear shallow-shell theory to obtain the equations of motion. In this study, nonlinear analysis was carried out by using energy approach.

The kinetic energy (T) and strain energy (U) of a circular cylindrical shell, by neglecting rotary inertia but retaining in-plane inertia, is given by:

$$T = \frac{1}{2}\rho_t \int_0^{2\pi}\int_0^{L}(\dot{u}^2 + \dot{v}^2 + \dot{w}^2)\, dxRd\theta \tag{37}$$

$$U = \frac{1}{2}\int_0^{2\pi}\int_0^{L}\{\varepsilon\}^T[S]\,\{\varepsilon\}dxRd\theta \tag{38}$$

The virtual work W done by the external forces is written as:

$$W = \int_0^{2\pi}\int_0^{L}(F_x u + F_\theta v + F_z w)dxRd\theta \tag{39}$$

Where F_x, F_θ and F_z are the distributed forces per unit area acting in axial, circumferential and radial directions, respectively.

In order to reduce the system to finite dimensions, the middle surface displacements u, v and w were expanded by using trial functions. The boundary conditions imposed at the shell ends, x = 0, L, are given by equation (23). According to these considerations, the displacements u, v and w were expanded by using the eigenmodes of the simply supported, empty shell:

$$u(x,\theta,t) = \sum_{m=1}^{i}\sum_{n=1}^{j} A_{mn}\cos(n\theta)\cos\left(\frac{m\pi x}{L}\right)T_{mn}(t) \tag{40}$$

$$v(x,\theta,t) = \sum_{m=1}^{i}\sum_{n=1}^{j} B_{mn}\sin(n\theta)\sin\left(\frac{m\pi x}{L}\right)T_{mn}(t) \tag{41}$$

$$w(x,\theta,t) = \sum_{m=1}^{i}\sum_{n=1}^{j} C_{mn}\cos(n\theta)\sin\left(\frac{m\pi x}{L}\right)T_{mn}(t) \tag{42}$$

Where A_{mn}, B_{mn} and C_{mn} are the linear mode shapes, which are obtained from free vibration analysis. $T_{mn}(t)$ are unknown functions which are dependent to time. The Lagrange equations of motion for the cylindrical shell are:

$$\frac{d}{dt}\left(\frac{\partial T}{\partial \dot{T}_{mn}(t)}\right) - \frac{\partial T}{\partial T_{mn}(t)} + \frac{\partial U}{\partial T_{mn}(t)} = \frac{\partial W}{\partial T_{mn}(t)} \qquad (m = 1..i, n = 1..j) \tag{43}$$

The set of nonlinear differential equation will be obtained from Eq. (42). The solution of these equations will be obtained by using numerical method.

5 Finite element modeling

For validating the result of nonlinear analysis the finite element modeling is proceed by ABAQUS software and the results of FEM are compared with analytical result. The FEM analysis is carried out according to nonlinear (large deflection) dynamic analysis in ABAQUS.

6 Results and discussion

To validate the analysis, results for simply supported cylindrical shells compared with Loy et al. [27], Table (1). The functionally gradient material (FGM) considered composed of stainless steel and nickel and its properties graded in the thickness direction according to a volume fraction power-law distribution. The comparisons show that the present results for the frequency characteristics agreed well with the Loy result.

Table 1 Comparison of natural frequency (Hz) with Loy (N=1, m=1, h/R=0.002, L/R=20)

	n=1	n=2	n=3	n=4	n=5	n=6	n=7	n=8	n=9	n=10
Present study	13.211	4.4799	4.1569	7.0383	11.241	16.455	22.635	29.771	37.861	46.904
Loy result	13.211	4.4742	4.1486	7.0330	11.238	16.453	22.633	29.770	37.861	46.904

In this section, the nonlinear vibrations of simply supported functionally graded circular cylindrical shells with different constituent volume fractions and configurations analyzed. The functionally graded material composed by stainless steel and nickel, its properties graded in the thickness direction according to a volume fraction distribution, where β is the considered power-law exponent. The material properties reported in Table (2).

Table 2 Properties of stainless steel and nickel

Stainless steel			nickel		
E (Nm^{-2})	ν	$\rho(kgm^{-3})$	E (Nm^{-2})	ν	$\rho(kgm^{-3})$
2.08×10^{11}	0.318	8166	2.05×10^{11}	0.31	8900

The circular cylindrical shell excited by means of an external modally distributed radial force, $F_z = 2\cos(2\pi \times 231.4 \times 0.998 \times t)$. It assumed that the force is exerted on the middle of shell $(x = L/2\,,\ \theta = 0)$. The amplitude-time response for middle point of a FGM shell with L=0.519 mm, R=149.4 mm and L=520 mm shown in figure (2). As shown in figure (2), the 18 number of degrees of freedom found to have a good accuracy for the nonlinear response.

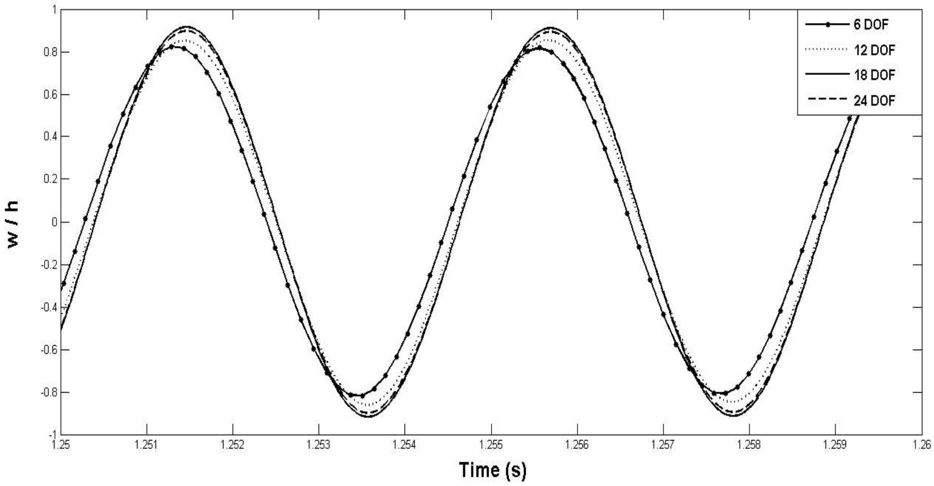

Figure 2 Comparison of nonlinear amplitude-time curves

(L=0.519 mm, R=149.4 mm, L=520,$\boldsymbol{\beta = 1}$)

In figure (3), a comparison of nonlinear amplitude-frequency curves of the FGM cylindrical shell shown: the nonlinear 6 dofs model describes a wrong hardening nonlinear behavior, the higher-order nonlinear expansions converge to a strongly softening nonlinear behavior, that is the correct character of the shell response.

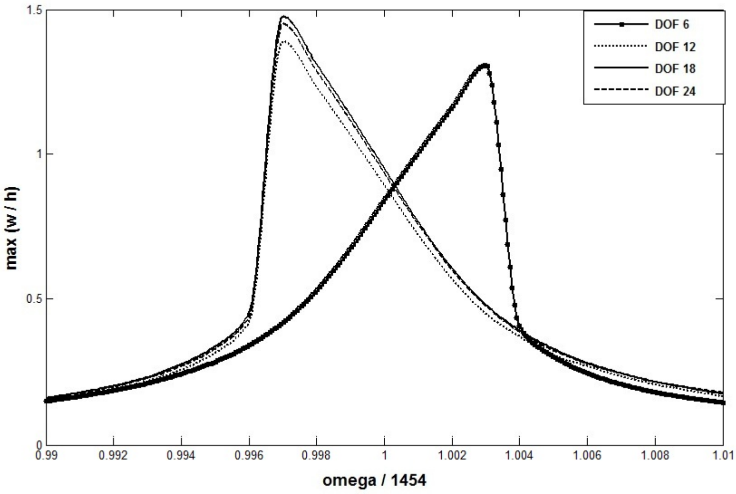

Figure 3 Comparison of nonlinear amplitude- frequency curves
(L=0.519 mm, R=149.4 mm, L=520,$\boldsymbol{\beta = 1}$)

In figure (4), a linear amplitude-frequency curve of the FGM cylindrical shell is shown. As shown in figure (4), the maximum of amplitude jumped at natural frequency of FGM cylindrical shell (231.4 Hz). That is, the correct character of the shell response for linear analysis.

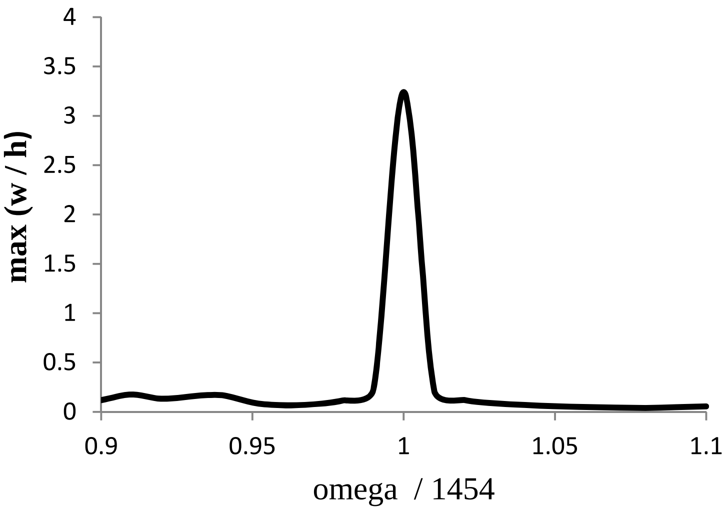

Figure 4 linear amplitude- frequency curves

(L=0.519 mm, R=149.4 mm, L=520,$\boldsymbol{\beta = 1}$)

In figure (5), it is found that by increasing the amplitude of excitation force the peak point of nonlinear amplitude-frequency curve moves to the left and the amplitude of radial displacement increased. So the effect of the nonlinearity (large deflection) can be obtained from figure (5) by increasing the amplitude of excitation force.

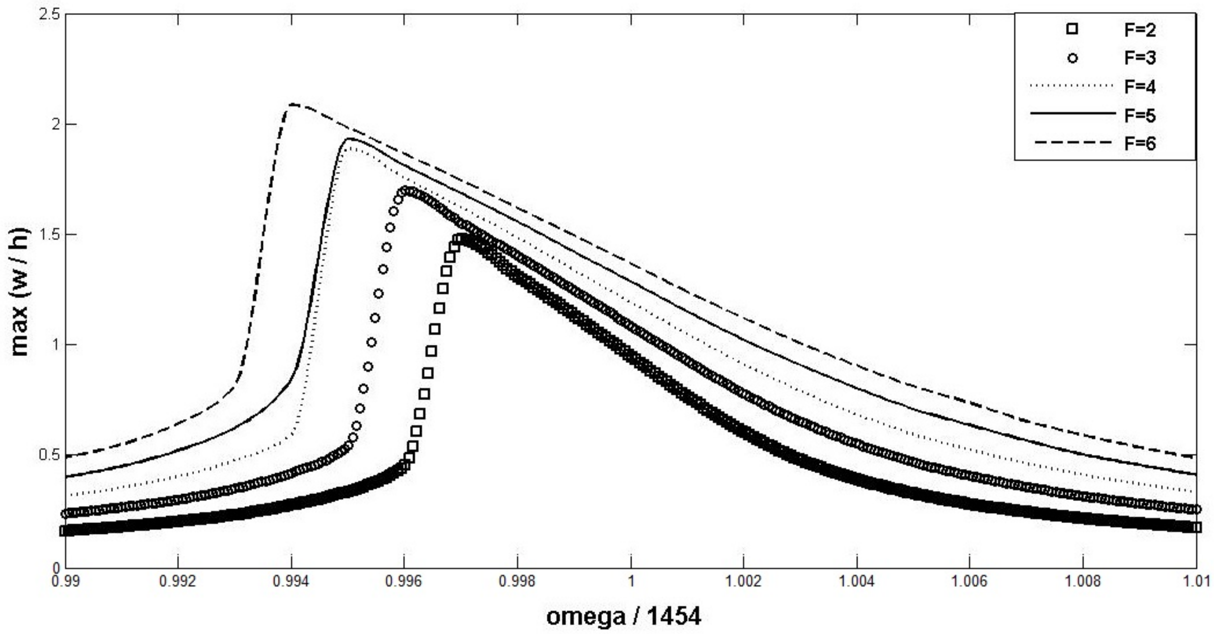

Figure 5 nonlinear amplitude- frequency curves for different amplitude of excitation force

(L=0.519 mm, R=149.4 mm, L=520,$\beta = 1$)

The time history of the radial displacement at the middle length of the cylindrical shell is shown in figure (6) for internal pressure loading. It is seen that with increasing the power law exponent ($\beta = N$) maximum deflection of curves move to the right and increase smoothly, because the portion of nickel and stainless steel is varied and result in changing the natural frequency of FGM shell.

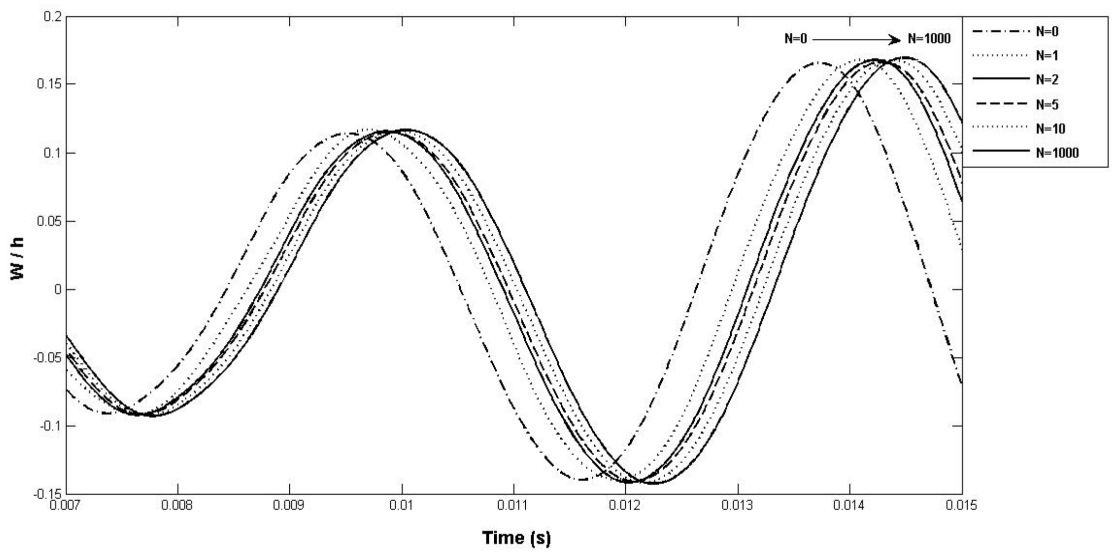

Figure 6 nonlinear time history of the radial displacement for different power law exponent of FGM material

For validation of analytical results, which were obtained from nonlinear analysis (large deformation assumption) the finite element model is developed by using ABAQUS software. The time history curve for both analytical and FEM are shown in figure (7) and (8). As seen in these figures, there is a good agreement between analytical and FEM analysis for nonlinear vibration of functionally graded cylindrical shell under harmonic radial load.

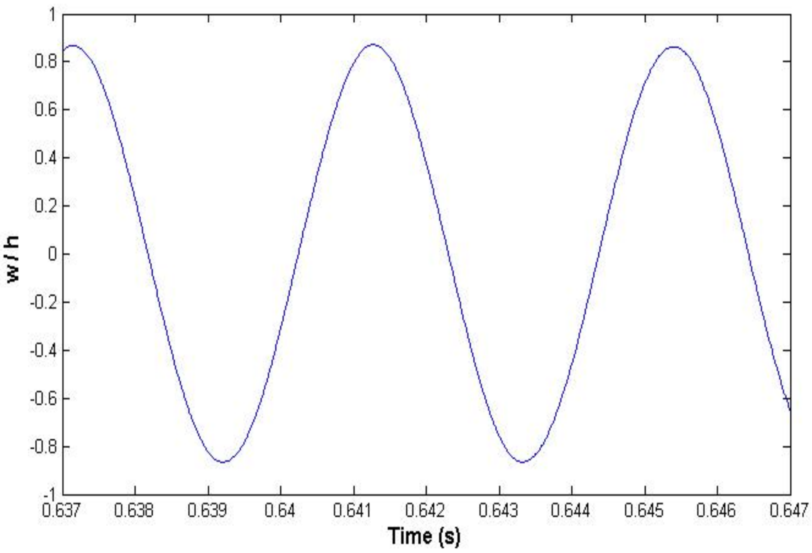

Figure 7 nonlinear amplitude-time curves from analytical analysis
(L=0.519 mm, R=149.4 mm, L=520,$\beta = 0$)

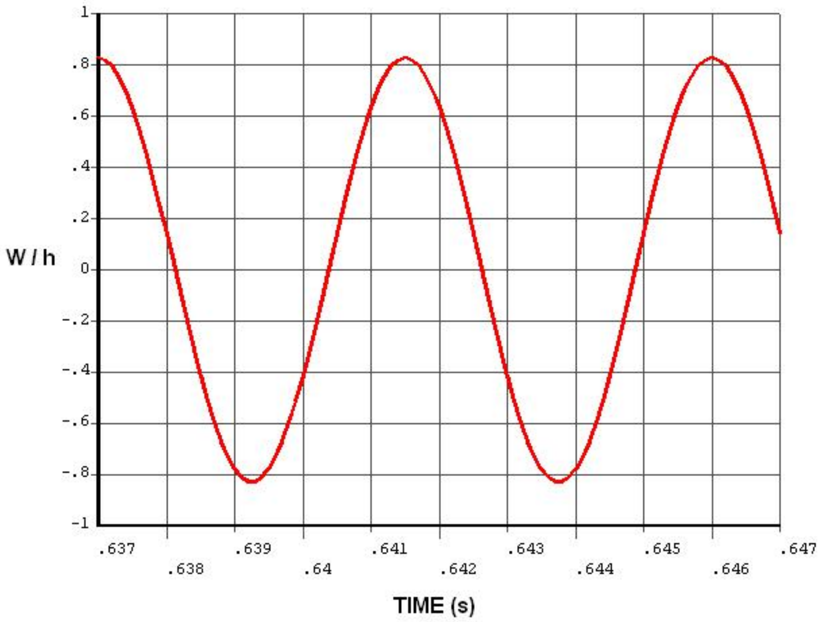

Figure 8 nonlinear amplitude-time curves from FEM model
(L=0.519 mm, R=149.4 mm, L=520, $\beta = 0$)

7 Conclusion

In this paper, the nonlinear vibrations of FGM circular cylindrical shells are analyzed. Different configurations and constituent volume fractions are considered. Nonlinear large deflection Donnell's theory is applied to model nonlinear dynamics of the system in the case of finite amplitude of vibration. The shell deformation is described in terms of longitudinal, circumferential and radial displacement fields. Simply supported boundary conditions are considered. Displacement fields are expanded by means of a double mixed series based on harmonic functions for the circumferential and longitudinal variable.

Numerical analyses are carried out in order to characterize the nonlinear response of the shells. A convergence analysis is developed by introducing in longitudinal, circumferential and radial displacement fields a different number of linear modes; the correct number of modes to describe the actual nonlinear behaviour of the cylindrical shells was determined. Frequency-response curves for both linear and nonlinear analysis were obtained and the effect of nonlinear terms was investigated via these curves. As shown in frequency-response curves, the softening behavior of nonlinear terms is due to the nonlinear terms in equations (Large deformation). Also the effect of external force was studied and by increasing the amplitude of external the peak of frequency-response curves move to the left and the amplitude of radial displacement is increased. In other words, by additional force the influence of nonlinear terms increased.

The influence of the constituent volume fractions and the effect of the configurations of the constituent materials on the natural frequencies and nonlinear responses of the shells were analyzed.

References

[1] Koizumi, M., "*FGM Activities in Japan*," Composites, (1997).

[2] Ghosh, A., Miyamoto, Y., Reimanis, I., and Lannutti, J.J., "Functionally Graded Materials, Manufacture, Properties and Applications. Ceramic Transactions", AM Ceram Soc, Vol. 76, pp. 171–89, (1997).

[3] Suresh, S., and Mortensen, A., "Functionally Gradient Metals and Metal Ceramic Composites", Part 2: Thermo Mechanical Behavior. Int. Mater, Vol. 42, pp. 85–116, (1997).

[4] Pindera, M.J., Arnold, S.M., and Abodi, J., "Use of Composites in Functionally Graded Materials", Compos Eng, Vol. 4, pp. 1–145, (1994).

[5] Yamanouchi, M., Koizumi, M., Hirai, T., and Shiota, I., "In: Proceedings of the First International Symposium on Functionally Gradient Materials", Japan, Sendai, (1990).

[6] Koizumi, M., "Functionally Gradient Materials the Concept of FGM", Ceram Trans, Vol. 34, pp. 3–10, (1993).

[7] Hiari, T., "*Functional Gradient Materials in Material Science and Technology*", Brook RJ, Editor. Processing of Ceramics, Part 2, Vol. 17B, pp. 293–341, (1996).

[8] Fukui, Y., "Fundamentals of Functionally Graded Materials", London: Institute of Materials, (1998).

[9] Yamaoka, H., Yuki, M., Tahara, K., Irisawa, T., Watanabe, R., and Kawasaki, A., "Fabrication of Functionally Gradient Material by Slurry Stacking and Sintering Process", Ceram Trans Funct Gradient Mater, pp. 169–72, (1993).

[10] Makino, A., Araki, N., Kitajima, H., and Ohashi, K., "Transient Temperature Response of Functionally Gradient Material Subjected to Partial Stepwise Heating", Trans JSME Part B, Vol. 60, pp. 4200–6, (1994).

[11] Obata, Y., and Noda, N., "Steady Thermal Stresses in a Hollow Circular Cylinder and a Hollow Sphere of a Functionally Gradient Material", J. Therm. Stresses, Vol. 17, pp. 471–87, (1994).

[12] Takezono, S., Tao, K., Inamura, E., and Inoue, M., "Thermal Stress and Deformation in Functionally Graded Material Shells of Revolution under Thermal Loading Due to Fluid", JSME Int. Ser. A: Mech. Mater. Eng. Vol. 39, pp. 573–81, (1994).

[13] Durodola, J.F., and Adlington, J.E., "Functionally Graded Material Properties for Disks and Rotors", In: Proceeding of the 1st International Conference on Ceramic and Metal Matrix Composites, San Sebastian, Spain, (1996).

[14] Dao, M., Gu, P., Maeqal, A., and Asaro, R., "A Micro Mechanical Study of a Residual Stress in Functionally Graded Materials", Acta Mater. Vol. 45, pp. 3265–76, (1997).

[15] Weisenbek, E., Pettermann, H.E., and Suresh, S., "Elasto-plastic Deformation of Compositionally Graded Metal-ceramic Composites", Acta Mater. Vol. 45, pp. 3401–17, (1997).

[16] Praveen, G.N., and Reddy, J.N., "Nonlinear Transient Thermoelastic Analysis of Functionally Graded Ceramic–metal Plates", International Journal of Solids and Structures, Vol. 35, pp. 4457–76, (1998).

[17] Park, J.S., and Kim, J.H., "Thermal Postbuckling and Vibration Analyses of Functionally Graded Plates", Journal of Sound and Vibration, Vol. 289, pp. 77–93, (2006).

[18] Yang, J., Liew, K.M., Wu, Y.F., and Kitipornchai, S., "Thermo-mechanical Post-buckling of FGM Cylindrical Panels with Temperature-dependent Properties", International Journal of Solid and Structures, Vol. 43, pp. 307–24, (2006).

[19] Reddy, J.N., "Analysis of Functionally Graded Plates", International Journal for Numerical Methods in Engineering, Vol. 47, pp. 663–84, (2000).

[20] Hosseini Kordkheili, S.A., and Naghdabadi, R., "Geometrically Nonlinear Thermoelastic Analysis of Functionally Graded Shells using Finite Element Method", International Journal for Numerical Methods in Engineering, Vol. 72, pp. 964–86, (2007).

[21] Arciniega, R.A., and Reddy, J.N., "Large Deformation Analysis of Functionally Graded Shells", International Journal of Solids and Structures, Vol. 44, pp. 2036–52, (2007).

[22] Woo, J., and Merguid, S.A., "Nonlinear Analysis of Functionally Graded Plates and Shallow Shells", International Journal of Solids and Structures, Vol. 38, pp. 7409–7421, (2001).

[23] Huaiwei, H., and Qiang, H., "Research on Nonlinear Postbuckling of Functionally Graded Cylindrical Shells under Radial Loads", Composite Structures, Vol. 92, pp. 1352–1357, (2010).

[24] Huaiwei, H., and Qiang, H., "Nonlinear Buckling of Torsion-loaded Functionally Graded Cylindrical Shells in Thermal Environment", European Journal of Mechanics A/Solids, Vol. 29, pp. 42–48, (2010).

[25] Ng, T.Y., Lam, K.Y., Liew, K.M., and Reddy, J.N., "Dynamic Stability Analysis of Functionally Graded Cylindrical Shells under Periodic Axial Loading", Int. J. Solids Structures, Vol. 38, pp. 1295–1309, (2001).

[26] Lam, K.Y., and Loy, C.T., "Influence of Boundary Conditions for a Thin Laminated Rotating Cylindrical Shells", Composite Structures, Vol. 41, pp. 215–228, (1998).

[27] Loy, C.T., Lam, K.Y., and Reddy, J.N., "Vibration of Functionally Graded Cylindrical Shell", Int. J. Mechanical Science, Vol. 41, pp. 309-324, (1999).

Nomenclature

F : material properties
V : volume fraction of FGM
β : power law exponent
h : thickness of shell
L : length of shell
R : radios of shell
E : elastic modulus
ν : Poisson's ratio
$N_x, N_\theta, N_{x\theta}$: force resultants
$M_x, M_\theta, M_{x\theta}$: moment resultants
u, v, w : displacements vectors in x, θ, z direction respectively
x, θ, z : directions of coordinate systme
e_x, e_θ, $e_{x\theta}$: strain components of the middle surface
ω_{mn} : natural frequency
F_x, F_θ, F_z : external loads
K_{ij}, M_{ij} : stiffness and mass matrices
T : kinetic energy
U : strain energy
W : virtual work done by the external forces

چکیده

در این مقاله، ارتعاشات غیرخطی پوسته استوانه‌ای از جنس مواد هدفمند، تحت بارگذاری شعاعی هارمونیک، بررسی شده است. معادلات غیرخطی پوسته بر اساس تئوری غیرخطی پوسته نازک Donnell در نظر گرفته شده است، که بر اساس این تئوری، روابط غیر خطی ناشی از کرنش‌های von Karman می‌باشد.

معادلات حرکت با استفاده از روش انرژی و رابطه لاگرانژ بدست می‌آیند. در جهت حل مسئله تغییر مکان-های صفحه میانی بر اساس توابع سری فوریه در نظر گرفته شده است. ثوابت این توابع شامل شکل مودهای، بدست آمده از حل ارتعاشات آزاد خطی، می‌باشد. پاسخ زمانی و فرکانسی برای حالت خطی و غیر خطی بدست آمده‌اند. همچنین نتایج بدست آمده با نتایج نرم‌افزار المان محدود مقایسه شده‌اند.